ISSN 1001-6538
CN 11-1785/N

Volume 59 · Number 2 · January 2014

Chinese Academy of Sciences, National Natural Science Foundation of China

Chinese Science Bulletin

科学通报

www.scichina.com
csb.scichina.com
www.springer.com/scp
link.springer.com

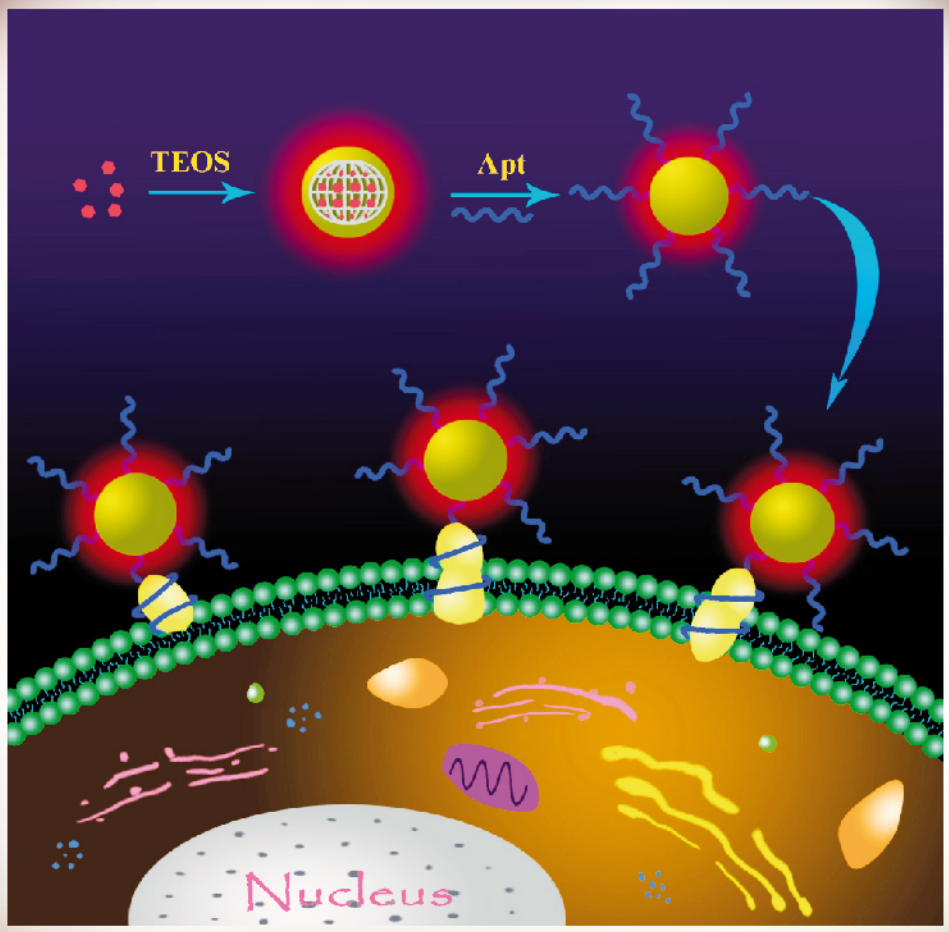

SCIENCE CHINA PRESS
Springer

Chinese Science Bulletin
Volume 59 ■ Number 2 ■ January 2014 ■ pp 113–238

Chinese Science Bulletin

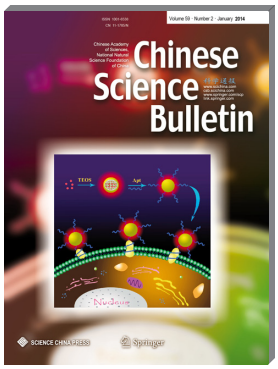

Volume 59 Number 2
January 2014

COVER Dye-doped silica nanoparticles (NPs) are used as optical biosensors and fluorescence imaging markers because of their chemical stability, facile surface modification and relatively high fluorescence quantum yield. Prions are responsible for the transmissible spongiform encephalopathies such as scrapie, "mad cow disease" or Creutzfeldt-Jakob disease. The cellular isoform of the prion protein (PrP^{C}) undergoes a conformational conversion to the insoluble pathogenic isoform (PrP^{Sc}). PrP^{C} is involved in cellular metabolism processes and its translocation is very important in the conversion of PrP^{Sc}. Cheng Zhi Huang's group from Southwest University (Chongqing, China) has developed a simple and sensitive method for imaging PrP^{C} by using an aptamer-labeled $Ru(bpy)_3^{2+}@SiO_2$ NP probe. Their optical probe possesses a long fluorescence lifetime (369.9 ns) and nearly no leakage of the dye from the silica matrix was observed (9 d after 12,000 r/min centrifuging for 15 min). The cover picture shows a fluorescence image of the probe targeting human bone marrow neuroblastoma cells (SK-N-SH cells) since they can express PrP^{C} on the surface. Moreover, $Ru(bpy)_3^{2+}@SiO_2$ NPs exhibit good biological compatibility, which make them ideally suited for long-term and real-time imaging of biological molecules (see the article by Wei Wang et al. on page 147).

Abstracted/indexed in:

Academic Search Alumni Edition
Academic Search Complete
Academic Search Elite
Academic Search Premier
ASFA 1: Biological Sciences and Living Resources
ASFA 2: Ocean Technology, Policy and Non-Living Resources
Biological Abstracts
Biological Sciences
BIOSIS Previews
CAB Abstracts
Chemical Abstracts
Chemical and Earth Sciences
Current Contents/Physical
Current Mathematical Publications
Digital Mathematics Registry
EMBio
Environmental Engineering Abstracts
Environmental Sciences and Pollution Management
Google Scholar
Inspec
Mathematical Reviews
MathSciNet
Meteorological and Geoastrophysical Abstracts
Pollution Abstracts
Science Citation Index
SCOPUS
Water Resources Abstracts
Zentralblatt MATH
Zoological Record

Go To Website

Volume 59 Number 2 January 2014

CONTENTS

REVIEW

ARTICLES

CONTENTS

Chinese Science Bulletin Vol. 59 No. 2 January 15, 2014 (Published three times every month)

Supervised by Chinese Academy of Sciences
Sponsored by Chinese Academy of Sciences and National Natural Science Foundation of China
Published by Science China Press and Springer-Verlag Berlin Heidelberg
Subscriptions
China Science China Press, 16 Donghuangchenggen North Street, Beijing 100717, China
Email: sales@scichina.org Fax: 86-10-64016350
North and South America Springer New York, Inc., Journal Fulfillment, P.O. Box 2485, Secaucus, NJ 07096 USA
Email: journals-ny@springer.com Fax: 1-201-348-4505
Outside North and South America Springer Customer Service Center, Customer Service Journals, Haberstr. 7, 69126 Heidelberg, Germany
Email: subscriptions@springer.com Fax: 49-6221-345-4229
Printed by Beijing Artownprinting Co., Ltd., Chuangyeyuan Road, Taihu Town, Tongzhou District, Beijing 101116, China
Edited by Editorial Board of Chinese Science Bulletin, 16 Donghuangchenggen North Street, Beijing 100717, China
Editor General Zuoyan Zhu

CN 11-1785/N
广告经营许可证: 京东工商广字第0429号

邮发代号: 80-214 (英)
国内每期定价: 120元

Chin. Sci. Bull. (2014) 59(2):133–137
DOI 10.1007/s11434-013-0035-2

csb.scichina.com
www.springer.com/scp

Article

Condensed Matter Physics

Antilocalization sensing of interactions between two-dimensional electrons and surface species

Yao Zhang · Victoria Soghomonian · Raymond L. Kallaher · Jean J. Heremans

Received: 30 August 2013 / Accepted: 12 October 2013 / Published online: 28 December 2013

Abstract We apply antilocalization measurements to experimentally study the interactions and exchange between InAs surface accumulation electrons and local magnetic moments of the rare earth ions Sm^{3+}, Gd^{3+}, Ho^{3+}, and Dy^{3+}, of the transition metal ions Ni^{2+}, Co^{2+}, and Fe^{3+}, and of Fe_3O_4 nanoparticles and Fe^{3+}-phthalocyanine deposited on the surface. The influence of the deposited species on the surface electrons is observed through the changes in the spin–orbit scattering and magnetic spin-flip scattering rates, which carry information about magnetic interactions. Experiments indicate a temperature-dependent magnetic spin-flip scattering for Ho^{3+}, Dy^{3+}, Ni^{2+}, and Co^{2+}. Concerning the spin–orbit scattering rate, we observe an increase, except for the cases of Ni^{2+}, Fe^{3+}, Fe_3O_4 nanoparticles and Fe^{3+}-phthalocyanine. We also observe an increase in SO scattering in another system where we study the interactions of Au nanoparticles and ferromagnetic $Co_{0.6}Fe_{0.4}$ nanopillars and an $In_{0.53}Ga_{0.47}As$ quantum well. Experimental results are analyzed and compared to theoretical models. Our method provides a controlled way to probe the quantum properties of two-dimensional electron systems, either on the surface of InAs or in a quantum well.

Keywords Antilocalization · Magnetoresistance · Magnetism · Surface states · Spin–orbit interaction · Spin-flip scattering

Y. Zhang · V. Soghomonian · R. L. Kallaher · J. J. Heremans (✉)
Department of Physics, Virginia Tech, Blacksburg, VA 24061, USA
e-mail: heremans@vt.edu

1 Introduction

Low-temperature weak-localization (WL) and weak antilocalization (AL) magnetotransport measurements are sensitive to electron interference, and thus can be used as a probe of quantum states [1–5]. The spin–dependent interactions between controllable surface magnetism and itinerant electrons in a non-magnetic host provide insight for spin-based technologies, magnetic data storage and quantum information processing. We study two different host systems, a two-dimensional electron system (2DES) on an InAs surface, and an InGaAs quantum well at a distance from the surface of a heterostructure. In a series of comparative AL measurements, we study the interactions between the 2DES and various species, magnetic or otherwise, deposited on the surface. The spin decoherence of a 2DES can be modified due to the presence of local spin moments. Therefore, by AL the interactions and spin exchange mechanisms between electrons and surface magnetic moments can be investigated in this adjustable artificial structure.

Interference between backscattered time-reversed electron trajectories contributes to the quantum corrections of the conductivity. In situations where the spin–orbit interaction (SOI) is absent, the constructive interference decreases the conductivity, resulting in WL [6]. In materials with strong SOI, the interference becomes destructive, and thus an increase in conductivity is observed known as AL [6, 7]. The InAs epitaxial layer has prominent Rashba SOI due to structural inversion asymmetry, and hence shows AL, with a sharp positive magnetoresistance (MR) around zero magnetic field ($B = 0$) applied normal to the surface, which crosses over to negative MR at higher B. This characteristic MR due to the AL quantum corrections to the two-dimensional conductivity $\sigma_2(B)$ is determined

by four scattering times: the elastic scattering time τ_0 (independently determined by carrier mobility and density); the inelastic decoherence time τ_i; the spin–orbit decoherence time τ_{SO}; and the magnetic spin-flip decoherence time τ_s. In our experiments, τ_s contains all the important information about the interactions between surface local moments and the 2DES. An expression for $\Delta\sigma_2(B) = \sigma_2(B) - \sigma_2(B=0)$ can be obtained through several theories, for instance developed by Hikami Larkin and Nagaoka (HLN) [7], or by Iordanskii Lyanda-Geller, and Pikus (ILP) [8]. HLN theory assumes spin–orbit scattering only at impurity sites, while ILP theory allows for the inclusion of SOI terms from the crystal structure or heterostructure, and is the preferred theory of choice when D'yakonov–Perel' spin relaxation mechanism is dominant. However, in our low mobility materials and at low temperatures, the spin scattering is dominated by the Elliott–Yafet mechanism. In this mechanism, the origin of the spin–orbit scattering is less important; it may be due to structural SOI combined with orbital scattering at impurity sites (as in our case), or due to spin–orbit scattering only locally at impurities. To properly express the interactions in our studies, we adopt the HLN expression simplified from the ILP model [8], and obtain Eq. (1) with the following modifications. In the presence of the spin-flip scattering, the phase coherence time τ_ϕ will be replaced by $\tau_\phi^{-1} = \tau_i^{-1} + 2\tau_s^{-1}$ [9, 10], and τ_{SO}^{-1} by $\tau_{SO}^{-1} - \tau_s^{-1}$ [10], which yields:

$$\begin{aligned}\Delta\sigma_2(B) = &\frac{e^2}{2\pi^2\hbar}\left\{-\left[\psi\left(\frac{1}{2}+\frac{B_0}{|B|}\right)-\psi\left(\frac{1}{2}+\frac{B_i+B_{SO}+B_s}{|B|}\right)\right.\right.\\ &+\frac{1}{2}\psi\left(\frac{1}{2}+\frac{B_i+2B_s}{|B|}\right)-\frac{1}{2}\psi\left(\frac{1}{2}+\frac{B_i+2B_{SO}}{|B|}\right)\Bigg].\\ &+\left[\ln\left(\frac{B_0}{|B|}\right)-\ln\left(\frac{B_i+B_{SO}+B_s}{|B|}\right)\right.\\ &\left.\left.+\frac{1}{2}\ln\left(\frac{B_i+2B_s}{|B|}\right)+\frac{1}{2}\ln\left(\frac{B_i+2B_{SO}}{|B|}\right)\right]\right\},\end{aligned} \tag{1}$$

where $\psi(x)$ is the digamma function and each decoherence time τ_α (with $\alpha = 0$, i, SO, s) corresponds to a characteristic magnetic field $B_\alpha = \hbar/(4eD\tau_\alpha)$, with D being the two-dimensional diffusion constant.

2 Experimental

We study the interaction of surface species and their interactions with InAs surface and with quantum wells in an InGaAs heterostructure. In the case of the InAs samples, consisting of 3.75 μmm thick *n*-InAs films grown on GaAs (001) substrates through metal organic chemical vapor deposition, we pattern two immediately neighboring twin serpentines, as shown in Fig. 1. The serpentines enhance the observed signal by increasing the channel length (8,820 μm) to width (40 μm) ratio. The presence of twin serpentines allows for comparative measurements, where one serpentine is left bare and the other covered by the following species: aqueous nitrate solution of rare earth (RE) ions (6×10^{-4} M), aqueous nitrate solutions of transition metal (TM) ions (6×10^{-4} M), and an aqueous polymer decorated Fe_3O_4 nanoparticle solution of $\sim 6 \times 10^{-4}$ M. In the case of Fe^{3+}-phthalocyanine, one of the serpentines was covered with phthalocyanine (not left bare). Both compounds were dissolved in chloroform with a concentration of $\sim 10^{-4}$ M. A 0.01 μL of any solution is deposited on one of a pair of serpentines, and then air dried (outlined in Fig. 1). We estimate the surface species density on the order of 10^{-6} μm^{-2}. The twin serpentines are fabricated simultaneously on the same sample and experience the same fabrication processes and cooldown. Thus the measured AL signal differences will be due only to the presence of surface magnetic species and their interactions with the 2DES.

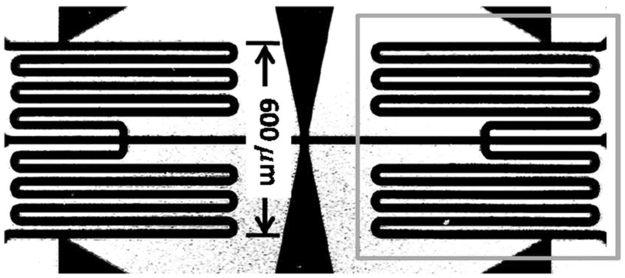

Fig. 1 (Color online) Structure of a sample, two identical serpentines are adjacent to each other. *Right* serpentine is covered by surface species (within the *square outline*); *Left* is bare for comparative measurements

The InGaAs quantum well, located at 19 nm from the surface of the following heterostructure is another system probed by our comparative AL measurements. The heterostructure, grown by molecular-beam epitaxy on semi-insulating InP (001) substrate, consists of a 500 nm $In_{0.52}Al_{0.48}As$ buffer, a 6 nm $In_{0.52}Al_{0.48}As$ doping layer, a 7 nm $In_{0.52}Al_{0.48}As$ layer, the 10 nm wide $In_{0.53}Ga_{0.47}As$ QW, a 17 nm $In_{0.52}Al_{0.48}As$ layer, and a 2 nm undoped InP cap layer. We study two surface species here: Au nanoparticles deposited from an aqueous solution and ferromagnetic CoFe nanopillars delineated by electron beam lithography and grown by thermal evaporation. We deposit 0.01 μL of 10^{-8} M of Au nanoparticles, with average particle size of 10 nm. The CoFe nanopillars, 40 nm in diameter and 36 nm in height, are arranged in a square array with minimum center to center distance of 200 nm. As in the case of InAs, comparative measurements are obtained between twinned bare and covered serpentines at low temperatures. Measurements occur by standard four-

contact low-frequency lock-in techniques, at cryogenic temperatures (0.4–6 K), and under variable B always applied normal to the surface.

3 Results and discussion

Before we discuss the details of the various systems we use the case of RE ions on InAs to demonstrate the effect of the surface magnetic moments. We compare the low-B AL data obtained on bare versus RE ion covered mesas on InAs at temperature $T = 0.4$ K (Fig. 2a, b). An expression of $\Delta R(B)/R_0$ is applied to present the MR, where $\Delta R(B) = R(B) - R(B = 0)$, $R_0 = R(B = 0)$, and R stands for the longitudinal resistance. Since $\Delta R(B) \ll R_0$, with $\Delta\sigma_2(B)/\sigma_2(B = 0) \approx -\Delta R(B)/R_0$, experimental $R(B)$ values can be directly compared to Eq. (1). To eliminate the effect from the external electronic shifts like Hall effect, the data is symmetrized. From Fig. 2 evaluating the data for the RE InAs sample, it is apparent that RE ions raise and broaden the AL signal, demonstrating the sensitivity of AL to surface species.

3.1 InAs with RE ions

From Hall data we measure areal density $N_s \sim 0.6\times 10^{12}$ cm^{-2} and $\mu \sim 22{,}000$ cm^2/Vs. Accounting for non-parabolicity in the InAs conduction band, with a Γ-point effective mass of 0.024 and a low T band gap of 418 meV, other transport parameters, such as τ_0 and D, are derived [1]. For a given sample, mobilities and densities do not vary in the range of the experimental T. Further, no significant systematic variation caused by solution coverage is observed. Information about the interaction between the surface moments and the surface electrons is extracted from the comparative (rather than absolute) AL data, and presented as spin-flip scattering rates τ_s^{-1}as function of T. We have shown that the RE ions (Sm^{3+}, Gd^{3+}, and Ho^{3+}) strongly influence τ_s^{-1} [1]. While Sm^{3+} and Gd^{3+} cause a T-independent τ_s^{-1} scaling with their effective moments μ_{eff}, Ho^{3+} shows a dependence $\tau_s^{-1} \sim T^n$ with $n \approx \frac{1}{2}$. The origin for the $\tau_s^{-1} \sim T^{1/2}$ observed for InAs electrons interacting with Ho^{3+} may be due to high μ_{eff} and large number of low-lying energy levels from nonzero orbital quantum number L. Based on values of L and μ_{eff} of a rare earth species, one may predict its behavior and interaction with itinerant electrons. For example, Dy^{3+} possesses a nonzero L and a fairly large μ_{eff} similar to that of Ho^{3+}, and thus an increase in τ_s^{-1} as T increases is expected, and was in fact observed. At $T = 0.4$ and 1.3 K, the spin-flip scattering of the serpentine covered with Dy^{3+} ions is derived to be 0.07 and 0.11 ps^{-1}, respectively, demonstrating the expected T-dependence of τ_s^{-1}.

3.2 InAs with TM ions

While the RE ions have buried 4f shell electrons responsible for their paramagnetic behavior, the TM ions have their outermost (and not buried) 3d shell electrons responsible for their magnetic properties. Using the same InAs surfaces, we expect stronger interactions between TM ions and the accumulation electrons. Figure 3 shows a good correspondence between data and theoretical fits for both bare and covered serpentines of the TM InAs samples at $T = 0.4$ K. By fitting Eq. (1) to the AL data of the TM InAs samples, temperature dependent spin-flip scattering is observed for both Ni^{2+} and Co^{2+}, and the dependence scales with the μ_{eff} of the magnetic ions. Similar to Ho^{3+}, both Ni^{2+} and Co^{2+} possess a high μ_{eff} and a nonzero L.

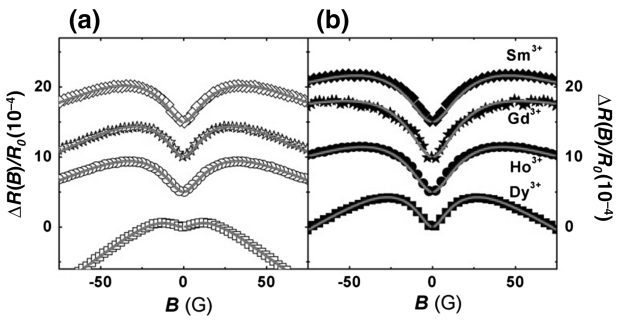

Fig. 2 (Color online) **a** Antilocalization measurements of the bare serpentines (*empty symbols*) paired with the serpentines covered by the RE magnetic species (*solid symbols*) in (**b**) at $T = 0.4$ K. **b** Antilocalization measurements of the serpentines covered by magnetic species paired with the bare serpentines in (**a**) at $T = 0.4$ K. (For clarity, only 1 in 6 experimental data are plotted, and an offset of 5×10^{-4} is applied on *curves*). The magnetic species are Sm^{3+} (*diamonds*), Gd^{3+} (*stars*), Ho^{3+} (*circles*), and Dy^3 (*squares*). *Solid lines* are from fitting

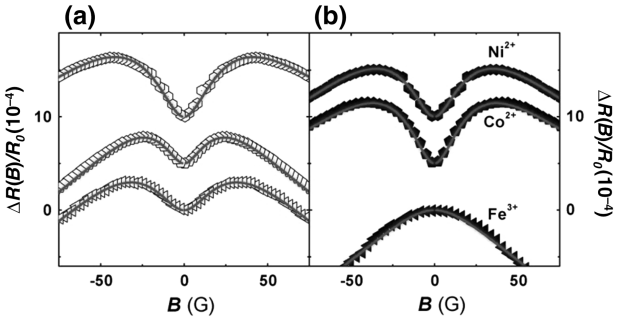

Fig. 3 (Color online) **a** Antilocalization measurements of the bare serpentines (*empty symbols*) paired with the serpentines covered by magnetic species (*solid symbols*) in (**b**) at $T = 0.4$ K. **b** Antilocalization measurements of the serpentines covered by magnetic species paired with the bare serpentines in (**a**) at $T = 0.4$ K. (For clarity, only 1 in 6 experimental data are plotted, and an offset of 5×10^{-4} is applied on *curves*). Magnetic species are Ni^{2+} (*hexagons*), Co^{2+} (*pentagons*), and Fe^{3+} (*triangles*). *Solid lines* are from fitting

On the other hand, for Fe^{3+} $L = 0$ and a T-independent τ_s^{-1} is observed as expected. Spin–orbit scattering, which carries information about the strength of the SOI is altered by the TM ions in various ways differently than in the case of the RE ions. While Co^{2+} broadens the AL signal, Ni^{2+} and Fe^{3+}reduce the signal. Particularly in the case of Fe^{3+} ions, the AL signal is in fact changed into WL. We attribute this to SOI possibly being suppressed by ferromagnetic ordering on the surface [11]. Or, the high spin-flip scattering of the Fe^{3+} ions may cause fast spin decoherence and thus mask the SOI.

3.3 InAs with Fe_3O_4 nanoparticles and Fe^{3+}-phthalocyanine

The significant change to the AL signal observed for Fe^{3+} ions may allow probing the interaction of distant local magnetic moments with surface electrons. We investigated other compounds containing this ion; decorated Fe_3O_4 nanoparticles and Fe^{3+}-phthalocyanine. In the case of the aqueous nitrate Fe^{3+}, the iron ions are in close proximity to the InAs surface electrons. With the decorated nanoparticles, firstly, we have a combination of Fe^{2+} and Fe^{3+}, and secondly, the diameter of the PPO/PEO decorated nanoparticle is $\sim$40 nm, of which only a central sphere of $\sim$8 nm is the Fe_3O_4. Thus, the iron oxide nanoparticles are at some distance from the surface, on the order of $\sim$10 nm. In the case of the Fe^{3+}-phthalocyanine, we surmise that the phthalocyanine molecule sits either flat or at a slight angle to the surface, and thus the Fe^{3+} ion is in relative proximity to the surface. Similar amounts of Fe_3O_4 nanoparticles and Fe^{3+}-phthalocyanine molecules were deposited onto two separate InAs samples. The comparative measurements of low-B AL at $T = 0.4$ K is shown in Fig. 4. Qualitatively, Fig. 4 indicates a decrease in AL signal for both samples, which confirms that the Fe^{3+} ions suppress the SOI. The reduced interaction between magnetic species and electrons can be still probed by the AL measurement, even when the Fe^{3+} ions are at some distance from the surface.

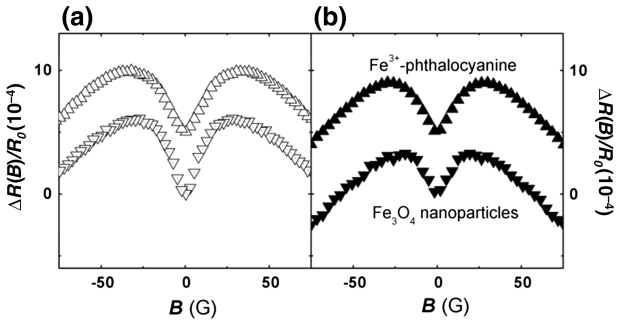

Fig. 4 **a** At $T = 0.4$ K, the antilocalization measurement of the serpentine covered by phthalocyanine (*empty up triangles*) paired with the serpentine covered by Fe^{3+}-phthalocyanine (*solid up triangles*) in (**b**); and the antilocalization measurements of the bare serpentine (*empty down triangles*) paired with the serpentine covered by Fe_3O_4 nanoparticles (*solid down triangles*) in (**b**). **b** At $T = 0.4$ K, the antilocalization measurement of the serpentine covered by covered by Fe^{3+}-phthalocyanine paired with the serpentine covered by phthalocyanine in (**a**); and the antilocalization measurement of the serpentine covered by Fe_3O_4 nanoparticles paired with the bare serpentine in (**a**). (For clarity, only 1 in 6 experimental data are plotted, and an offset of 5×10^{-4} is applied on *curves*)

3.4 InGaAs with Au nanoparticles and $Co_{0.6}Fe_{0.4}$ nanopillars

The feasibility of probing magnetic moments within a reasonable distance may allow us to apply AL measurement to a quantum well buried in a heterostructure, at a certain distance from the surface. In the heterostructure studied, the InGaAs 2DES is situated at 19 nm from the surface. In the first case, we have a magnetic CoFe nanopillar array on a serpentine twinned with a bare serpentine. In a comparative AL measurement, we find that the presence of the magnetic nanopillars generates a pseudo-random magnetic field that the QW electrons experience as an effective SOI. In the second case, we deposited 0.01 μL solution of 10^{-8} M 10 nm Au nanoparticles on one of a pair of serpentines on the surface of the heterostructure, while the other is left bare for comparative measurements. While Au is non-magnetic, due to its heavy atomic mass (high Z) Au can induce strong spin–orbit scattering. Figure 5 shows the comparative measurements for both the CoFe nanopillars and the Au nanoparticles, and we note the good correspondence between theoretical fits and the AL data at $T = 0.4$ K. By fitting Eq. (1) to the data, without modifying the inelastic decoherence time τ_i, the Au nanoparticles decrease the τ_{SO}. Therefore, the SOI is

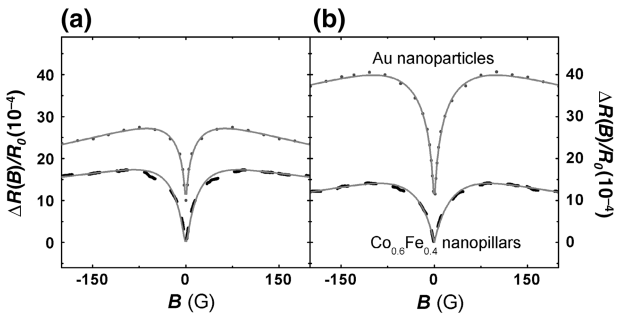

Fig. 5 (Color online) **a** Antilocalization measurements of the bare serpentines paired with the serpentines covered by surface species in (**b**) at $T = 0.4$ K. **b** Antilocalization measurements of the serpentines covered by surface species paired with the bare serpentines in (**a**) at $T = 0.4$ K. (For clarity, only 1 in 6 experimental data are plotted, and an offset of 0.01 is applied on *curves*). Surface species are Au nanoparticles (*dot lines*) and $Co_{0.6}Fe_{0.4}$ nanopillars (*dash lines*). *Solid lines* are from fitting

increased as expected. From Fig. 5, we notice that the CoFe nanopillars behave differently than the other magnetic species; the AL signal is broadened, but also lowered at the same time. The increased SOI is attributed to the presence of a pseudo-random magnetic field component due to the fringing magnetic field of the nanopillars. The reduced depth of the signal is from an average fringing field normal to the heterostructure surface. The results with the QW indicate the effectiveness of AL measurements in probing interactions of surface local moments and electron systems even at a distance.

4 Conclusions

We demonstrate that antilocalization measurements are indeed a sensitive probe to study spin–dependent interactions between surface local moments and two-dimensional systems, even in a buried quantum well. Almost all the surface species studied here were deposited from solution, providing an easy route to generating tunable structures. Our antilocalization results allow for predictions regarding the behavior of magnetic ions on itinerant electron systems. Further, we illustrate the value of including spin-flip scattering into the known analytical expressions of the quantum corrections to the classical conductivity, and provide support through our antilocalization measurements on a variety of distinct situations.

Acknowledgments The authors thank Prof. Judy Riffle for providing the decorated Fe_3O_4 nanoparticles. The work was supported by the U.S. Department of Energy, Office of Basic Energy Sciences, Division of Materials Sciences and Engineering under Award (DOE DE-FG02-08ER46532).

References

1. Zhang Y, Kallaher RL, Soghomonian V et al (2013) Measurement by antilocalization of interactions between InAs surface electrons and magnetic surface species. Phys Rev B 87:054430
2. Wei W, Bergmann G (1988) CuCo: a new surface Kondo system. Phys Rev B 37:5990–5993
3. Gang T, Deniz Yilmaz M, Atac D et al (2012) Tunable doping of a metal with molecular spins. Nat Nanotechnol 7:232–236
4. He HT, Wang G, Zhang T et al (2011) Impurity effect on weak antilocalization in the topological insulator Bi_2Te_3. Phys Rev Lett 106:166805
5. Lu HZ, Shi JR, Shen SQ (2011) Competition between weak localization and antilocalization in topological surface states. Phys Rev Lett 107:076801
6. Bergmann G (1984) Weak localization in thin films: a time-of-flight experiment with conduction electrons. Phys Rep 107:1–58
7. Hikami S, Larkin AI, Nagaoka Y (1980) Spin–orbit interaction and magnetoresistance in the two dimensional random system. Prog Theor Phys 63:707–710
8. Iordanskii SV, Lyanda-Geller YB, Pikus GE (1994) Weak localization in quantum wells with spin–orbit interaction. Pis'ma Zh Eksp Teor Fiz 60:199–203
9. Haesendonck CV, Vranken J, Bruynseraede Y (1987) Resonant Kondo scattering of weakly localized electrons. Phys Rev Lett 58:1968–1971
10. Licini JC, Dolan GJ, Bishop DJ (1985) Weakly localized behavior in quasi-one-dimensional Li films. Phys Rev Lett 54:1585–1588
11. Dugaev VK, Bruno P, Barnas J (2001) Weak localization in ferromagnets with spin–orbit interaction. Phys Rev B 64:144423


Special Topic:
Spectral Analysis
Effects of lactic acid on stem cells
SPECIAL ISSUE
Extreme Climate in China
SCIENCE CHINA PRESS
Springer
SpringerOpen
Chinese Science Bulletin
Genome analysis of the caterpillar fungus
Electrostatic analysis of the face-to-face dimer interface
Alveolar remodeling in Jurassic theropods
Chinese Science Bulletin
2013 Cover Gallery
Submit Your Cover Images to CSB
SCIENCE CHINA
CHINESE SCIENCE BULLETIN
WWW.SCICHINA.COM
SCIENCE CHINA PRESS
Emotion regulation explored by ERP
ARK methods for gaseous detonation simulation
Isolation of a novel brittle culm gene
DNMTs and chromosomes in oocytes of aging mice
Biosorption and biodegradation of PAHs

SCIENCE CHINA
CHINESE SCIENCE BULLETIN
WWW.SCICHINA.COM
SCIENCE CHINA PRESS

For more information, please visit the journal website at

http://csb.scichina.com DOWNLOAD

Chinese Science Bulletin

A multidisciplinary scientific journal
Published three times every month

Print ISSN: 1001-6538
Online ISSN: 1861-9541

- Peer-reviewed
- Online submission
- Indexed by SCI, CA, etc.
- Professional and quick publication
- Pub ASAP

Editorial Office

Address:
16 Donghuangchenggen North Street, Beijing 100717, China
Tel: +86-10-64036120 | **Fax**: +86-10-64016350
Email: csb@scichina.org

Sponsored by
Chinese Academy of Sciences (CAS)
National Natural Science Foundation of China (NSFC)

Published by
Science China Press & Springer

ISSN 1001-6538